

Metastable localization of diseases in complex networks

R. S. Ferreira,¹ R. A. da Costa,² S. N. Dorogovtsev,^{2,3} and J. F. F. Mendes²

¹*Departamento de Ciências Exatas e Aplicadas, Universidade Federal de Ouro Preto, 35931-008 João Monlevade, Brazil*

²*Department of Physics & I3N, University of Aveiro, 3810-193 Aveiro, Portugal*

³*A. F. Ioffe Physico-Technical Institute, 194021 St. Petersburg, Russia*

We describe the phenomenon of localization in the epidemic SIS model on highly heterogeneous networks in which strongly connected nodes (hubs) play the role of centers of localization. We find that in this model the localized states below the epidemic threshold are metastable. The longevity and scale of the metastable outbreaks do not show a sharp localization transition, instead there is a smooth crossover from localized to delocalized states as we approach the epidemic threshold from below. Analyzing these long-lasting local outbreaks for a random regular graph with a hub, we show how this localization can be detected from the shape of the distribution of the number of infective nodes.

PACS numbers: 64.60.aq, 05.10.-a, 05.40.-a, 05.50.+q

I. INTRODUCTION

Localization is one of the key phenomena in nature. It was extensively explored in a wide range of systems including localization of electrons in disordered systems, localization of phonons, and many others [1–7]. Recently it attracted much attention in application to epidemic spreading [8, 9], where localization means persistence of an island of disease below the epidemic threshold around a strongly connected node or a dense cluster in a network. The complication is that the SIS (susceptible-infective-susceptible) epidemic model has an absorbing state in which infection is absent [10–12], and so below the epidemic threshold islands of disease with a finite number of infective nodes cannot survive forever. In other words, a system with a finite number of infected nodes has a non-zero probability to recover immediately. For a large but finite number of infected nodes, however, this probability is small, so the complete recovery can take a long time. For finite fully connected graphs, this behavior was described in Ref. [13]. Consequently, in the heterogeneous SIS model, localization should be only metastable [14], manifesting itself in the form of long-lasting local outbreaks of the disease below the epidemic threshold.

In this paper we consider the SIS model on a random regular graph with a single hub (“spreader center”) and investigate the metastable nature of localization of a disease. On a regular network, the SIS model is equivalent to the ordinary contact process [11] that belongs to the directed percolation universality class [15–17]. These processes can be solved exactly only on fully connected graphs, so we have to resort to extensive numerical simulations. On the other hand, the heterogeneous (annealed) [18, 19] and quenched [8, 19–21] mean-field approaches do not take into account the fluctuations and the absorbing state in the SIS model, so they cannot provide even a qualitative description of metastable localization. In the present paper we show how the effect of this localization can be detected by analyzing the shape of the distribution of the number of infected nodes in the metastable state. By metastable state we

mean the active quasistationary state below the epidemic threshold. Measuring the lifetime of the localized states we describe how the metastable localization depends on the epidemic parameter λ . From the distribution of the number of infective nodes in finite graphs we extract the contribution of the metastable localized states and compare it with the solution of the SIS model on a star graph, uncovering the effect of the network substrate. We observe two regimes, localized and delocalized, separated by a smooth crossover occurring in a region around $\lambda_{\text{crossover}} < \lambda_c$. Surprisingly, in contrast to predictions of the quenched mean-field theory, the disease is localized on a hub below the crossover region, and between $\lambda_{\text{crossover}}$ and λ_c , the effect of hub disappears.

II. MODEL

We study the SIS model on a random regular graph of N nodes, with all but one having degree k . The single hub in this graph is a node with $q \gg k$ connections. For the sake of comparison we also consider the same network without hub ($q = k$). The graph has finite length loops (cycles) only when N is finite.

In the SIS model, each node can be in two states: susceptible and infective. A susceptible node is infected by each of its infective nearest neighbors with rate λ (so-called effective spreading rate), which is the control parameter in this model. An infective node spontaneously recovers with unit rate. Our simulations for uniform networks up to 2×10^9 nodes confirmed that in the infinite random regular graph with the coordination number $k = 6$, the epidemic threshold is $\lambda_c = 0.2026(1)$ Ref. [22]. This is the usual continuous transition in the contact process above the upper critical dimension [11, 15–17, 23–25].

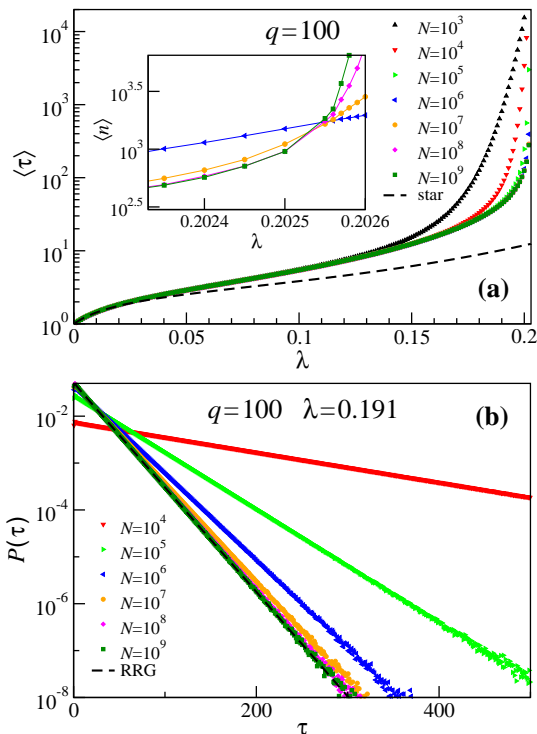


FIG. 1. Time to reach the absorbing state of the process for the random regular networks, $k = 6$, with a single hub of degree $q = 100$ below the epidemic threshold $\lambda_c = 0.2026(1)$. (a) Average lifetime of the process vs. λ when each realization starts from the state in which only the hub is infective (spreading experiment). For small λ , the curves approach the dependence $\langle \tau \rangle(\lambda)$ obtained from Eq. (4) for the corresponding star graph (dashed curve). The inset shows the average number of infective nodes in the spreading experiment near the epidemic threshold. (b) The distribution of times between the attempts to fall into the absorbing state in quasistationary simulations at $\lambda = 0.191 < \lambda_c$. The dashed line stands for the uniform network (random regular graph), $q = k = 6$.

III. SIMULATIONS

The SIS dynamics is implemented as follows [26, 27]. During the process we trace the numbers of infective nodes, $n(t)$, and of active links, $\ell(t)$. By definition, an active link is a link of an infective node, and the links between two infective nodes are counted twice in $\ell(t)$. At each step, with probability $n(t)/[n(t) + \lambda\ell(t)]$ a uniformly randomly chosen infective node becomes susceptible. With complementary probability $\lambda\ell(t)/[n(t) + \lambda\ell(t)]$ an active link is chosen uniformly at random. If it connects infective and susceptible nodes, then the susceptible one becomes infective. If both nodes are infective, nothing occurs. Finally, time is incremented by $1/[n(t) + \lambda\ell(t)]$.

We perform numerical simulations in two ways. In the first approach, which we call spreading experiment, in each realization, the hub is initially infective and the other nodes are susceptible, and the process finishes when

it reaches the absorbing state (all nodes susceptible). In the second approach, we obtain the quasistationary distribution of active nodes by the method of Refs. [28–30] that excludes the absorbing state from the simulations. When the SIS process reaches the absorbing state, we restore one of the previous active configuration taken at random from the history of the process. This procedure optimizes the numerical simulations confining the dynamics of the process to active states, which enables us to efficiently collect the statistics of the quasistationary regime independently on initial conditions. For more details about our simulation method see the Appendix.

Figure 1 presents the statistics for the lifetime of the process obtained by implementing these two approaches. In Fig. 1(a) we show the average time to reach the absorbing state (average lifetime) in the spreading experiment versus the parameter λ for different network sizes N . In the infinite network, the lifetime diverges at the epidemic threshold. For λ sufficiently small, all curves for different N collapse into one. As λ increases, these curves separate from each other due to the loops of a finite length which are present in the finite networks. These loops increase the average lifetime due to the additional reinfection of the hub occurring when disease spreads through a loop. In the locally tree-like infinite networks, loops are infinite, and reinfection is possible by only returning to the hub through the same path. The effect of loops is stronger in the small networks, and the curves start to separate at smaller λ as N decreases. The inset of Fig. 1(a) demonstrates a strong size effect on the average number of infective nodes $\langle n \rangle$ near the epidemic threshold. The average $\langle n \rangle$ in Fig. 1(a) is taken over the entire time of the spreading experiment and over realizations. In the quasistationary simulations, the lifetime of the process can be extracted from the distribution of times between the attempts to reach the absorbing state, see Fig. 1(b) for $\lambda = 0.191 < \lambda_c$. The figure shows that this distribution approaches the exponential distribution for a random regular graph as the network size goes to infinity.

Figure 2 shows how the average number of infective nodes $\langle n \rangle$ and the average lifetime $\langle \tau \rangle$ in the quasistationary regime depend on λ for different hub degrees and network sizes. We observe a strong dependence of $\langle n \rangle$ and $\langle \tau \rangle$ on q for λ below $\lambda_{\text{crossover}}(N, q)$. In this range of λ , $\langle n \rangle$ and $\langle \tau \rangle$ rapidly grow with q , which indicates that the disease is localized around a hub and survives for much longer times than in the homogeneous network. Above $\lambda_{\text{crossover}}$, the effect of the hub disappears, and the curves $\langle n \rangle(\lambda)$ and $\langle \tau \rangle(\lambda)$ collapse to the ones for the uniform random regular graph. The inset of Fig. 2(a) demonstrates that there is not a sharp transition from the localized state to delocalization but rather a smooth crossover between the two regimes. The dependence of $\langle n \rangle$ on the network size is well seen only in the region of this crossover. Notably, the curves $\langle n \rangle(\lambda)$ show a pronounced peak near $\lambda_{\text{crossover}}$ in contrast to $\langle \tau \rangle(\lambda)$. Finally, the inset of Fig. 2(b) depicts $\langle \tau \rangle$ for small λ , where

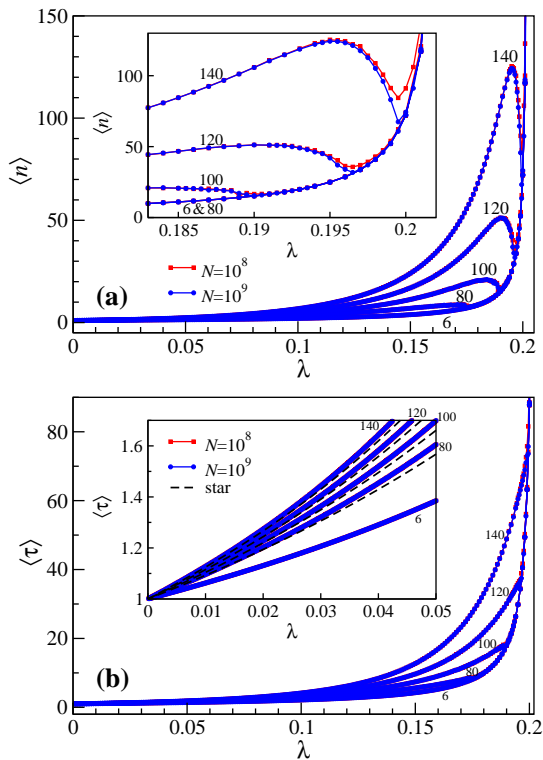


FIG. 2. (a) Average number of infective nodes $\langle n \rangle$ and (b) the average lifetime $\langle \tau \rangle$ in the quasistationary regime of the SIS model on random regular graphs with a single hub vs. $\lambda < \lambda_c \approx 0.2026$. The coordination number of the graph is 6. The curves are for two network sizes, 10^8 and 10^9 nodes, and different values of the hub degree q (see the numbers on the curves). The inset of panel (a) shows separation of the curves for networks of 10^8 and 10^9 nodes in the crossover region for each given q . The inset of panel (b) shows the region of small λ in which the curves are close to the solutions of Eq. (4) (dashed lines) for the corresponding star graphs with q leaves.

the results of the simulations are close to the lifetimes of the corresponding star graphs with q leaves.

To quantify the effect of the hub we consider the complete quasistationary distribution of the number of infective nodes, p_n . This distribution is the probability that at a random instant an active system contains n infective nodes. Figure 3(a),(c),(e) shows the distributions p_n for different hub degrees q . For each q , we choose the epidemic parameter λ in the corresponding crossover region, and measure p_n for different network sizes. For the sake of comparison, we show p_n for the random regular graph. The insets in these panels demonstrate a significant separation of these curves at large n (log-linear plots). To validate our results, we checked that p_1 perfectly agrees with the inverse first moment of the distribution $P(\tau)$, which is a fundamental relation [31].

IV. DECOMPOSITION OF THE DISTRIBUTION

The effect of a hub is local, which results in the contribution of the order of $1/N$ to full distribution p_n for large networks. Let us extract this contribution from the measured distribution $p_n(\lambda, q, N)$ for networks of different sizes by assuming the following ansatz:

$$p_n = A(N) \left[p_{n,k} + \frac{H_n}{N} \right], \quad (1)$$

where $p_{n,k}$ is the distribution of the number of infective nodes in the uniform random regular networks with coordination number k , H_n is a yet unknown function, and $A(N) = [1 + \sum_n H_n/N]^{-1}$ is a normalization factor. In this ansatz, H_n is independent of N in the limit of large N and is determined only by λ , k , and q . We first assume the form of Eq. (1) and then we shall validate it analyzing results of our simulations. The rationale behind this form is the following. As the network size goes to infinity, the region where activation of infective nodes is influenced by the hub remains finite. This region is the same as for the Bethe lattice with a hub. On the other hand, far away from the hub, active states in the quasistationary regime are similar to those for the uniform random regular graph, this area grows as N , and so the activity occurs mostly far from the hub. Consequently one can expect that the relative contribution of the localized states for the total distribution p_n indeed scales as $1/N$.

The direct application of Eq. (1) to extracting the function H_n from the numerical data obtained in our simulations for p_n and $p_{n,k}$ requires the knowledge of the normalization factor $A(N)$. We remove this unknown factor from the calculations by rewriting Eq. (1) as

$$\frac{p_{n+1}}{p_n} = \frac{p_{n+1,k} + H_{n+1}/N}{p_{n,k} + H_n/N}. \quad (2)$$

Using this equation we express H_{n+1} in terms of H_n and the distributions p_n and $p_{n,k}$,

$$H_{n+1} = [Np_{n,k} + H_n] \frac{p_{n+1}}{p_n} - Np_{n+1,k}. \quad (3)$$

For a given λ and an arbitrary initial value H_1 , we can extract the function H_n by iteratively applying this recursive equation to the numerical data for different N . The value H_1 is found by requiring that it provides the best collapse of the curves $H_n(N)$ into one for our set of sufficiently large network sizes N . (We repeat the calculations for different H_1 and select the value giving the best collapse of the curves.) Figure 3(b),(d),(f) shows that for each considered case, such a value H_1 exists, and the curves H_n obtained for different N collapse into one. Thus, the ansatz of Eq. (1) is correct, and for large N the function H_n is indeed independent of N . The existence of the function H_n indicates the presence of the metastable localized state in the system.

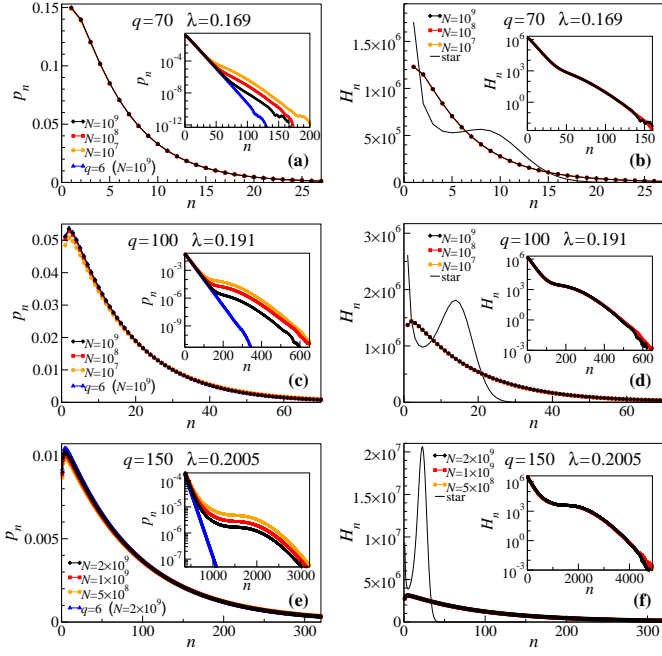


FIG. 3. (a), (c), and (e) Distribution p_n of the number of infective nodes in the quasistationary regime for different hub degree q and values of λ in the crossover region. Three different network sizes are presented in each panel. These plots also show the curves for uniform random regular graphs $q = k = 6$. The insets demonstrate the separation of these curves in log-linear representation. (b), (d), and (f) Curves H_n extracted from p_n by employing Eq. (3). The initial values $H_1 = 1.2 \times 10^6$, 1.4×10^6 and 2.7×10^6 in (b), (d), and (f), respectively, enable the collapse of the curves for different network sizes into one in each of the panels. The thin black lines show the stationary distributions p_n^{star} for the corresponding star graphs multiplied by $\sum_n H_n$ for the sake of comparison. The insets demonstrate the collapse of the curves of the main panels in log-linear representation.

Equation (1) explains the crossover between two regimes in Fig. 2 for different system sizes and hub degrees. In the localized regime $\sum_n H_n/N \gg 1$, so the distribution p_n is determined by the function H_n (note the normalization $\sum_n p_{n,k} = 1$ for the distribution $p_{n,k}$ of the number of infective nodes in a uniform random regular graph). This localized regime takes place in the region $0 < \lambda \lesssim \lambda_{\text{crossover}}(q, N)$. On the other hand, the delocalized distribution p_n coincides with $p_{n,k}$ because $\sum_n H_n/N \ll 1$ in the region $\lambda_{\text{crossover}}(q, N) \lesssim \lambda < \lambda_c$. The crossover between the localized and delocalized states takes place in the region around $\lambda_{\text{crossover}}(q, N)$, where $\sum_n H_n/N \sim 1$. So we define $\lambda_{\text{crossover}}$ as the value of λ for which $\sum_n H_n/N = 1$, clearly depending on N and q . One can see from Eq. (1) that the average number of active nodes $\langle n \rangle$ in our network consists of two parts:

$$\langle n \rangle = A(N)\langle n \rangle_k + [1 - A(N)]\langle n \rangle_H.$$

The first term is the bulk contribution, where $\langle n \rangle_k$ is for a uniform random regular graph. The second term is the

contribution of the hub, where $\langle n \rangle_H = \sum_n n H_n / \sum_n H_n$ represents the number of active nodes averaged over localized states. Both $\langle n \rangle_k$ and $\langle n \rangle_H$ are independent of N . As $N \rightarrow \infty$ the coefficient A approaches 1, and $\langle n \rangle$ approaches $\langle n \rangle_k$, on the other hand, for $N \ll \sum_n H_n$ the coefficient $A \ll 1$ and $\langle n \rangle \approx \langle n \rangle_H$.

Let us compare the function H_n with the distribution p_n^{star} of the number of infective nodes in the solution of the SIS model for the star graph of the same degree as the hub. Estimates for the recovery rate of the SIS model on a star were obtained in Ref. [26]. We cannot use them, since for our comparison we have to describe the evolution of this system completely, which can be done by implementing the approach of Ref. [13] used for solving the SIS model on a finite fully connected graph. The state of our system at moment t is given by the probability $P_{s,m}(t)$ that the central node is in state s ($s = 0, 1$ is for susceptible and infective, respectively) and m leaves are infective, where $0 \leq m \leq q$. The evolution of this probability is exactly described by the following equations:

$$\begin{aligned} \partial_t P_{0,m}(t) &= -(\lambda+1)mP_{0,m}(t) + (m+1)P_{0,m+1}(t) + P_{1,m}(t), \\ \partial_t P_{1,m}(t) &= -[\lambda(q-m)+m+1]P_{1,m}(t) + (m+1)P_{1,m+1}(t) \\ &\quad + \lambda(q-m+1)P_{1,m-1}(t) + \lambda m P_{0,m}(t), \end{aligned} \quad (4)$$

with the boundary conditions $P_{0,q+1}(t) = P_{1,-1}(t) = P_{1,q+1}(t) = 0$. These equations describe the Markov chain in Fig. 4. The initial conditions are $P_{1,0}(0) = 1$ and $P_{0,m}(0) = P_{1,m>0}(0) = 0$, i.e., we start with only the central node infective. The distribution of the number of infective nodes in a system with at least one infective node, $p_n^{\text{star}} = [P_{1,n-1}(t) + P_{0,n}(t)]/[1 - P_{0,0}(t)]$, becomes stationary for large t . This stationary distribution corresponds to the one obtained in our measurements in the quasistationary regime. We obtain p_n^{star} by numerically solving Eq. (4), which can be done with any desired precision for a finite q . Figure 3(b),(d),(f) shows the stationary distributions p_n^{star} for the stars with 70, 100, and 150 leaves multiplied, for the sake of comparison, by the constant $\sum_n H_n$ (thin solid curves). The difference between p_n^{star} and H_n is that in the star graph the dynamics is constrained to the hub and its nearest-neighbors, while the function H_n is determined by the network activity in a wider area around the hub.

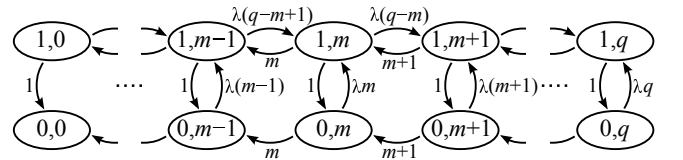


FIG. 4. Graphical representation of Eq. (4) for the SIS model on a star graph. The circles represent individual states and arrows show possible transitions between them. The number near each arrow denotes the rate of the transition.

V. DISCUSSIONS AND CONCLUSIONS

We have studied the localization of the disease in the SIS model on a random regular graph with a hub below the epidemic threshold. We found that the localized states in this system are metastable even in the infinite network limit due to the presence of the absorbing state in the SIS model. We have developed a method enabling us to quantify this phenomenon in large networks by analyzing the data of quasistationary simulations for networks of different sizes, specifically, the distributions of the number of infective nodes. We found a smooth crossover from localization on a hub at $0 < \lambda \lesssim \lambda_{\text{crossover}}(q, N)$ to the delocalized state in the region $\lambda_{\text{crossover}}(q, N) \lesssim \lambda < \lambda_c$. This is quite opposite to the quenched mean-field theory, in which localization on a hub is predicted above a certain value of $\lambda < \lambda_c$. Note that for a fixed $\lambda < \lambda_c$, there is also a crossover from a delocalized to a localized state as we increase the hub degree q . We completely described the distribution of the number of infective nodes in the metastable state by the linear combination of two contributions: (i) from the uniform network and (ii) the effect of the hub, see Eq. (1). We have demonstrated how to extract the contribution of the hub, H_n , shown in Fig. 3. In the quasistationary state this contribution decays as $1/N$ asymptotically, which means that the effect of the hub disappears in the infinite system. We have compared the extracted contribution with the solution of the SIS model on a star graph having the same number of leaves as the hub in our system. The marked difference between H_n and the distribution p_n^{star} revealed the influence of a wide neighborhood of the hub in the infinite network. Notably, we considered a large network with a single hub, which could not influence the epidemic threshold λ_c . Sufficiently high concentration of strongly connected nodes (hubs) can seriously displace or even eliminate the epidemic threshold [26, 32].

We have characterized the phenomenon of metastable localization of a disease below the epidemic threshold in a model heterogeneous system and the crossover to a delocalized state. Our work revealed a drastic difference of this kind of localization from the standard one. Common intuition tells that a hub should be important near λ_c where it can keep an island of disease. We find that, on the contrary, the effect of the hub actually disappears near the epidemic threshold. We suggest that our findings can be qualitatively applicable to long-lasting local outbreaks in a wide range of epidemic processes with an absorbing state on highly heterogeneous networks.

ACKNOWLEDGMENTS

We thank G. J. Baxter, A. V. Goltsev, and G. Zampieri for many stimulating discussions. This work was supported by the FET proactive IP project MULTIPLEX 317532, and R.S.F. was supported by the

program Ciência sem Fronteiras—CAPES, grant No. 88881.030375/2013-01.

APPENDIX: SIMULATION OF THE QUASISTATIONARY STATE

Here we outline a few issues significant for our simulations.

(1) In finite networks of the kind under consideration, finite loops are present, which contribute to the reinfection of the hub, prolonging the localized activity, see Fig. 1(a). This contribution disappears in the infinite size limit. To ensure that our measurements are free from the effect of finite loops, for each combination of parameters λ and q we choose a set of network sizes in the range where the lifetime of the spreading experiment is already size independent, see collapse of curves in Fig. 1(a). For instance, in panels (e) and (f) of Fig. 3 we use larger system sizes than in the other panels because for $\lambda = 0.2005$ and $q = 150$ the effect of loops is observed for sizes $N \sim 10^8$.

(2) To access the quasistationary state we have to wait a long time after the start of the process. It is very likely that the system falls into the absorbing state during the transient period, and we would have to restart the process many times before one realization lasts enough to reach the quasistationary state. Below the epidemic threshold, this is a quite inefficient approach because most of the computation time is spent simulating the transient and not the quasistationary state.

To overcome this difficulty we use the quasistationary method [28–30]. Within this approach, when the system falls in the absorbing state, we restart it from an active configuration taken at random from the history of active configurations visited by the process. For this, we keep a database of a large number of active configurations, where, at random instants, we save the current configuration in a random position of the database. As the process proceeds, the database is repeatedly updated and relaxes until the process converges to a stationary state that is independent of the initial conditions. In the limits of large number of states in the database and long times intervals between consecutive updates, the stationary states of the quasistationary method converges to the one of the original process. These two limits are important. They ensure that the configurations in the database are uncorrelated.

The quasistationary method can be viewed as a clever way of simulating the whole ensemble of realizations of the process while collecting data from a single realization. The advantage is that when the observed realization falls in the absorbing state we choose another at random, among the ones still active, and start collecting data from that moment forward. After the initial relaxation period of the history database we collect data without interruptions, dramatically reducing the computation time

needed for gathering a representative statistics.

(3) For each q in Fig. 3 we measure localized activity over 2 orders of magnitude of system size (from 10^7 nodes to 10^9). We maximize the difference between curves for different N by selecting $\lambda \approx \lambda_{\text{crossover}}(N=10^7, q)$. Recall that at $\lambda_{\text{crossover}}(10^7, q)$, we have $\sum_n H_n/10^7 = 1$. For $N = 10^9$ the fraction of localized configurations in the history database is already small, roughly $1\% \approx \sum_n H_n/10^9$. Because of this smallness we keep a database large enough that the average number of localized configurations stored there is much larger than its fluctuations.

For these simulations we keep a database of 10^5 configurations. This number of configurations allows us to have on average about $0.01 \times 10^5 = 1000 \gg 1$ localized configurations in the networks of 10^9 nodes. At each time step we update a random position of the database with the current configuration with probability $0.1dt/\langle\tau\rangle$, where $dt = 1/[n(t) + \lambda l(t)]$ is the lifetime of the configuration (see main text). With this update probability the average time interval between consecutive updates is of roughly $10\langle\tau\rangle$. By comparing simulations with different update

intervals we found that, in all of the cases considered, the results for an average update interval of $10\langle\tau\rangle$ are indistinguishable from those obtained with longer update intervals. We only start to collect data after each position of the database has been updated at least 10^3 times, allowing for the full relaxation of the history record.

(4) In the quasistationary state, the rate at which the system falls in the absorbing configuration is $1/\langle\tau\rangle$. In the SIS model, this rate must be exactly equal to the probability of the active system having only one infective node, p_1 , multiplied by the rate at which the infective node spontaneously recovers, which is 1 in this case [30, 31]. Then to check if the resulting stationary data are correct (e.g., not spoiled by errors in the code), it is useful to compare $\langle\tau\rangle$ and $1/p_1$. These two numbers must be equal with a high precision increasing with the collected amount of data. In our simulations we verify this equality with up to 7 digits of precision. Note that for $\langle\tau\rangle = 1/p_1$ to hold we must measure time as a continuous variable, incrementing it by $dt = 1/[n(t) + \lambda l(t)]$ at each step, and define p_n as the fraction of the total time that the system spends in configurations with n active nodes.

-
- [1] P. W. Anderson, "Absence of diffusion in certain random lattices," *Phys. Rev.* **109**, 1492 (1958).
- [2] I. M. Lifshitz, "The energy spectrum of disordered systems," *Adv. Phys.* **13**, 483 (1964).
- [3] D. J. Thouless, "Electrons in disordered systems and the theory of localization," *Phys. Rep.* **13**, 93 (1974).
- [4] T. R. Kirkpatrick, "Localization of acoustic waves," *Phys. Rev. B* **31**, 5746 (1985).
- [5] L. Jahnke, J. W. Kantelhardt, R. Berkovits, and S. Havlin, "Wave localization in complex networks with high clustering," *Phys. Rev. Lett.* **101**, 175702 (2008).
- [6] G. Ódor, "Localization transition, Lifschitz tails, and rare-region effects in network models," *Phys. Rev. E* **90**, 032110 (2014).
- [7] R. Pastor-Satorras and C. Castellano, "Distinct types of eigenvector localization in networks," arXiv:1505.06024 (2015).
- [8] A. V. Goltsev, S. N. Dorogovtsev, J. G. Oliveira, and J. F. F. Mendes, "Localization and spreading of diseases in complex networks," *Phys. Rev. Lett.* **109**, 128702 (2012).
- [9] H. K. Lee, P.-S. Shim, and J. D. Noh, "Epidemic threshold of the susceptible-infected-susceptible model on complex networks," *Phys. Rev. E* **87**, 062812 (2013).
- [10] R. M. Anderson and R. M. May, *Infectious Diseases of Humans*, Vol. 1 (Oxford University Press, Oxford, 1991).
- [11] J. L. Cardy and P. Grassberger, "Epidemic models and percolation," *J. Phys. A: Mathematical and General* **18**, L267 (1985).
- [12] R. Pastor-Satorras, C. Castellano, P. Van Mieghem, and A. Vespignani, "Epidemic processes in complex networks," *Rev. Mod. Phys.* **87**, 925 (2015).
- [13] C. Deroulers and R. Monasson, "Field-theoretic approach to metastability in the contact process," *Phys. Rev. E* **69**, 016126 (2004).
- [14] F. D. Sahneh, A. Vajdi, and C. Scoglio, "Delocalized epidemics on graphs: A maximum entropy approach," arXiv preprint arXiv:1605.00198 (2016).
- [15] H. Hinrichsen, "Non-equilibrium critical phenomena and phase transitions into absorbing states," *Adv. Phys.* **49**, 815 (2000).
- [16] G. Ódor, "Universality classes in nonequilibrium lattice systems," *Rev. Mod. Phys.* **76**, 663 (2004).
- [17] M. Henkel, H. Hinrichsen, S. Lübeck, and M. Pleimling, *Non-equilibrium phase transitions*, Vol. 1 (Springer, 2008).
- [18] R. Pastor-Satorras and A. Vespignani, "Epidemic spreading in scale-free networks," *Phys. Rev. Lett.* **86**, 3200 (2001).
- [19] C. Castellano, "Theoretical approaches to the susceptible-infected-susceptible dynamics on complex networks: Mean-field theories and beyond," in *Nonlinear Phenomena in Complex Systems: From Nano to Macro Scale* (Springer Netherlands, 2014) p. 133.
- [20] P. Van Mieghem, "The n-intertwined sis epidemic network model," *Computing* **93**, 147 (2011).
- [21] P. Van Mieghem, "Epidemic phase transition of the sis type in networks," *EPL (Europhysics Letters)* **97**, 48004 (2012).
- [22] A. S. Mata and S. C. Ferreira, "Pair quenched mean-field theory for the susceptible-infected-susceptible model on complex networks," *EPL (Europhysics Letters)* **103**, 48003 (2013).
- [23] S. N. Dorogovtsev, A. V. Goltsev, and J. F. F. Mendes, "Critical phenomena in complex networks," *Rev. Mod. Phys.* **80**, 1275 (2008).
- [24] R. S. Ferreira and S. C. Ferreira, "Critical behavior of the contact process on small-world networks," *Eur. Phys. J. B* **86**, 1 (2013).
- [25] C.-R. Cai, Z.-X. Wu, M. Z. Q. Chen, P. Holme, and

- J.-Y. Guan, “Solving the dynamic correlation problem of the susceptible-infected-susceptible model on networks,” *Phys. Rev. Lett.* **116**, 258301 (2016).
- [26] M. Boguñá, C. Castellano, and R. Pastor-Satorras, “Nature of the epidemic threshold for the susceptible-infected-susceptible dynamics in networks,” *Phys. Rev. Lett.* **111**, 068701 (2013).
- [27] S. C. Ferreira, C. Castellano, and R. Pastor-Satorras, “Epidemic thresholds of the susceptible-infected-susceptible model on networks: A comparison of numerical and theoretical results,” *Phys. Rev. E* **86**, 041125 (2012).
- [28] S. C. Ferreira, R. S. Ferreira, C. Castellano, and R. Pastor-Satorras, “Quasistationary simulations of the contact process on quenched networks,” *Phys. Rev. E* **84**, 066102 (2011).
- [29] M. M. de Oliveira and R. Dickman, “Quasi-stationary simulation: the subcritical contact process,” *Braz. J. Phys.* **36**, 685 (2006).
- [30] M. M. de Oliveira and R. Dickman, “How to simulate the quasistationary state,” *Phys. Rev. E* **71**, 016129 (2005).
- [31] R. Dickman and R. Vidigal, “Quasi-stationary distributions for stochastic processes with an absorbing state,” *J. Phys. A: Mathematical and General* **35**, 1147 (2002).
- [32] S. C. Ferreira, R. S. Sander, and R. Pastor-Satorras, “Collective versus hub activation of epidemic phases on networks,” arXiv preprint arXiv:1512.00316 (2015).